Microfluidics for the spectroscopy of carbon nanotubes

Ilkka Pekkala

Master's thesis

University of Jyväskylä

Department of Physics

20.8.2013

Supervisors: Andreas Johansson

Mika Pettersson

Abstract

We have successfully finalized the process of creating small microfluidic channels on glass chips, having 4 inlet/outlet holes for liquid flow. The fabricated channel structures can be as complex as electron beam lithography can make them. Working channels have the minimum width and depth of 4 μm x 4 μm.

The microfluidics is controlled with Fluigent MFCS, enabling pressures up to 345 mbar. Liquid flow rates range from 40 pl/s up to 1.2 nl/s. Objects in such small channels still run with channel speeds of tens of micrometers or even millimeters per second. With a T-junction structure, droplets of water/oil can be formed and controlled.

The system is coupled with a Raman microscope, enabling at least the detection of carbon nanotubes inside the droplets. However, due to high channel speeds, the droplets need to be stationary to get good measurements. Carbon nanotubes also tend to form bundles and finally block the channels. Raman spectrum of multiple nanotubes was observed.

The stage is now set for further and more complex measurements. Due to its limitations, this system will so far stay only in small-scale research.

Preface

I had no idea what I was about to step into when I received the e-mail asking would I be interested in a Master's thesis project. Interested? Yes. Scared? Even more so. However, Andreas Johansson was a great instructor, patiently helping me with the biggest and the smallest of problems. Coupled with a multidisciplinary team of experts like Janne Ihalainen, Mika Pettersson, Pasi Myllyperkiö and towards the end Ján Borovský, it was a pleasure to be part of this project.

There were many more people contributing to this project in their own ways. As this would be a rather lengthy list, I would just like to give a big thank you to all personnel of NanoScience Center in the University of Jyväskylä. The laser group of Heikki Häkkänen deserves special thanks as they contributed directly to the fabrication of the samples through laser drilling.

Of course, friends and family were important in the process. The good and the bad times, you had to see and listen to them all. Just being there for me was enough, but once in a while somebody gave me a small idea or a suggestion, which was more than anyone could ask. So here it finally is, my months of successes and failures, crystallized into a single work.

Contents

Abstract i

Preface ii

1 Introduction 1

1.1 Carbon nanotubes 1

1.2 About microfluidics 3

1.3 Raman spectroscopy of carbon nanotubes 6

2 Fabrication of microfluidic channels 7

2.1 Glass and pretreatments 8

2.2 Metal mask 9

2.3 Electron beam lithography 9

2.4 Wet etching 11

2.5 Thermal fusion of glass slides 12

2.6 Alternative methods and trials 14

3 Microfluidics 16

3.1 Microfluidic setup 16

3.2 Flow speeds at different pressures 18

3.3 Droplet formation 19

4 Raman measurements 20

5 Conclusions 22

Bibliography 24

1 Introduction

The goal of this research is to obtain a possibility to manipulate and measure different materials within microfluidic channels. First we need to make the microfluidic channels and do it so that they are optically transparent. Afterwards we should master to control the fluid flow inside the channels and enable the formation of droplets of different materials inside the channel. Finally, coupling the setup with Raman microscope, we should be able to observe and measure objects inside the droplets.

Our objects inside the droplets will first be carbon nanotubes, but the system is designed so that it wouldn't be limited to them; the droplets could also house chemical or biological samples. Other applications for the system could be small scale reaction kinetics inside the droplets or perhaps the recognition of viruses (or parts of them). If the complexity of the microfluidic channels can be increased enough, this could lead into sorting of the materials after the measurement.

1.1 Carbon nanotubes

Carbon nanotubes have been under heavy research ever since they were found. Their unique and unusual properties make them an interesting material to be used in several fields including electronics and nanotechnology. Carbon nanotubes are basically a sheet of graphene, which has been rolled to form a cylinder. The way the rolling is made is defined by chiral vector

$$R = n \cdot a_1 + m \cdot a_2 \quad (1)$$

Where n and m are integers. If the integers are equal, the nanotube is called armchair; if the second is zero, it's called zigzag. Any other combination makes chiral nanotubes. The chirality vectors are described in Figure 1.

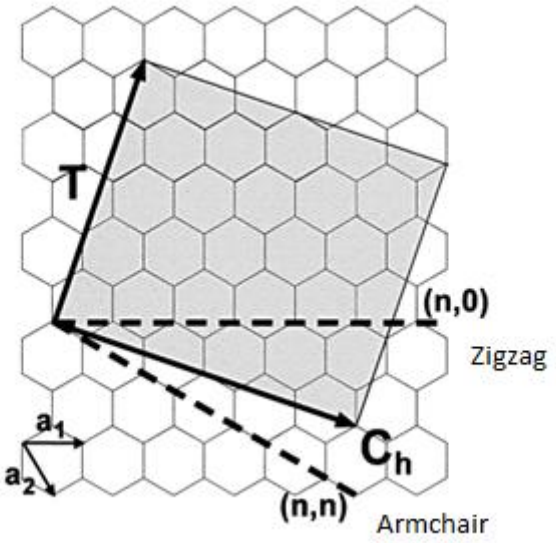

Figure 1 - Chiral vectors of a carbon nanotube [1]

The nanotubes are generally categorized as single-walled or multi-walled. If the nanotube consists of only one layer of rolled graphene, it is classified as single-walled. Any additional layers will result in its classification to multi-walled. The electric conductance of a nanotube self-explanatorily furthermore categorizes it into a semiconducting or metallic. Our main interests are single-walled nanotubes and the capability to distinguish metallic and semiconducting without actual electronic measurements. Figure 2 shows a single chiral nanotube, our main interest.

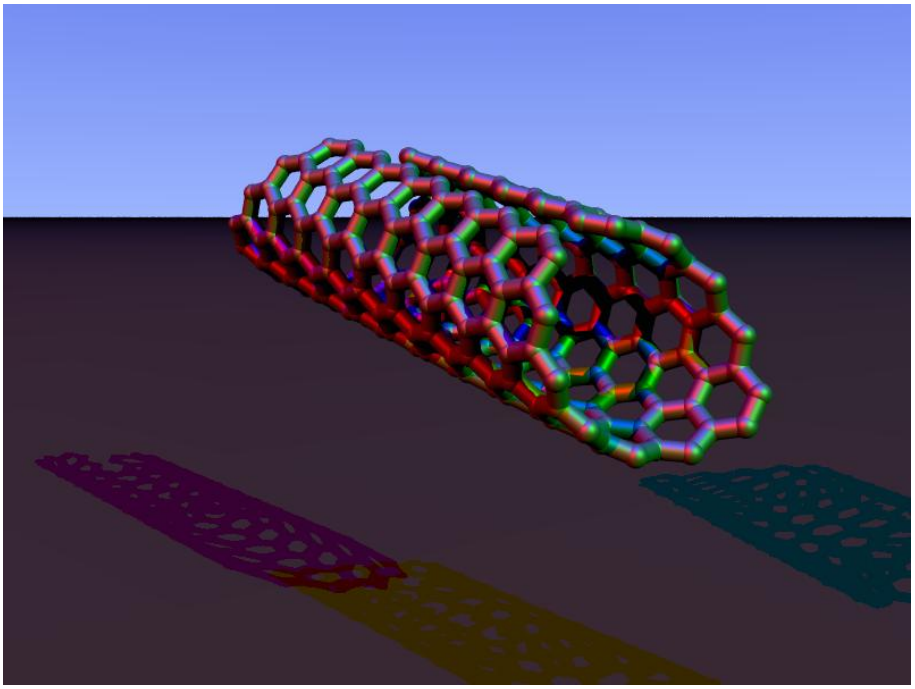

Figure 2- A single chiral nanotube[2]

Carbon nanotubes have a tendency to align themselves into ropes and bundles, not remaining as individuals for a long time. This causes some problems as in the path to understand carbon nanotubes better; it would be beneficial to observe only a single nanotube at a time. One long term goal of this project is to be able to isolate a single nanotube into one droplet and measure only that.

1.2 About microfluidics

In microfluidics the amounts of liquid used in the experiments are of very small volumes. Here we are attempting to reach picoliter or even femtoliter scales, and the liquid is constrained into micrometer-scale volumes of rectangular channels. The chan-

nels are fabricated into transparent soda-lime glass, which enables optical measurements such as Raman spectroscopy.

The measurement process with Raman microscope is not instantaneous, but takes a certain (although it may be small) amount of time. The droplets containing the carbon nanotubes should therefore move slowly enough so that the nanotube stays within the measurement zone for the duration of the measurement, or the liquid should be stoppable at will. This is why we are greatly interested in the flow rate of the liquid inside the channel. Considering a rectangular channel, the volume flow rate Q is

$$Q = \frac{C \cdot a \cdot b^3 \cdot \Delta p}{L \cdot \mu} = a \cdot b \cdot u \qquad (2)$$

Where C is the friction coefficient, μ the viscosity of the fluid, Δp the pressure difference and u the averaged velocity of the fluid inside the channel [3]. The terms a, b and L define the channel dimension as pictured in Figure 3.

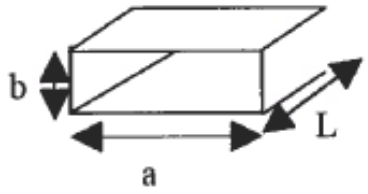

Figure 3 - Channel dimensions[3]

The friction coefficient C is slightly problematic as it is defined as

$$C = \frac{1}{2} \cdot \left(\frac{a}{b}\right)^2 \sum_{n=1}^{\infty} \frac{1}{\beta_n^4} \cdot \left[1 - \frac{1}{\beta_n} \cdot tanh\left(\beta_n \cdot \frac{a}{b}\right)\right] \quad (3)$$

With

$$\beta_n = \frac{(2 \cdot n - 1)}{2} \cdot \pi \quad (4)$$

To simplify this, a graphical representation of the dependence of C to the aspect ratio X = a/b is shown in Figure 4. Notice the logarithmic behavior of X.

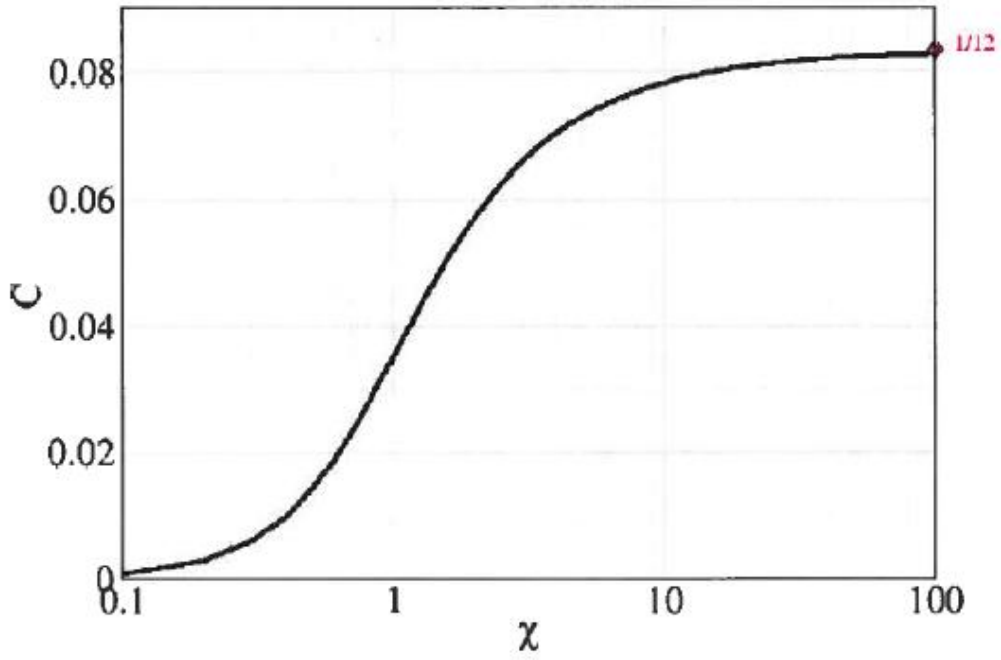

Figure 4 - Friction coefficient as a function of the aspect ratio[3]

An easier way to assess the flow rate of the liquid is to follow the flow under macroscopic conditions such that the friction and other microscopic properties are negligible. In a cylindrical tube the flow rate Q can be expressed as

$$Q = \frac{V_{cylinder}}{t} = \frac{\pi \cdot L}{t} \cdot \left(\frac{d}{2}\right)^2 \quad (5)$$

Where L is the length of the tube, d the inner diameter and t the time it takes to travel the distance.

Combining these equations allow us to evaluate the speed inside the channel by first observing the flow rate at macroscopic level and then calculating it inside the micro-fluidic channel, presuming we know the dimensions of the channel.

1.3 Raman spectroscopy of carbon nanotubes

When a beam of monochromatic light is shot to a molecule, a crystal, or even a carbon nanotube, a small fraction of the photons is scattered inelastically. These photons have either lower or higher frequency than the incident light beam, forming Stokes and anti-Stokes lines respectively. The Raman shift is conventionally expressed as wave number

$$\bar{\nu} = \frac{1}{\lambda_{incident}} + \frac{1}{\lambda_{scattered}} \quad (6)$$

Where λ is the wavelength of the light [4].

The ability to distinguish between semiconducting and metallic nanotubes comes with Raman spectroscopy. As seen in Figure 5, their Raman spectra are slightly different. Easiest way to distinguish between them is by looking at the G-band. Semiconducting nanotube has a much sharper peak whilst metallic has broader.

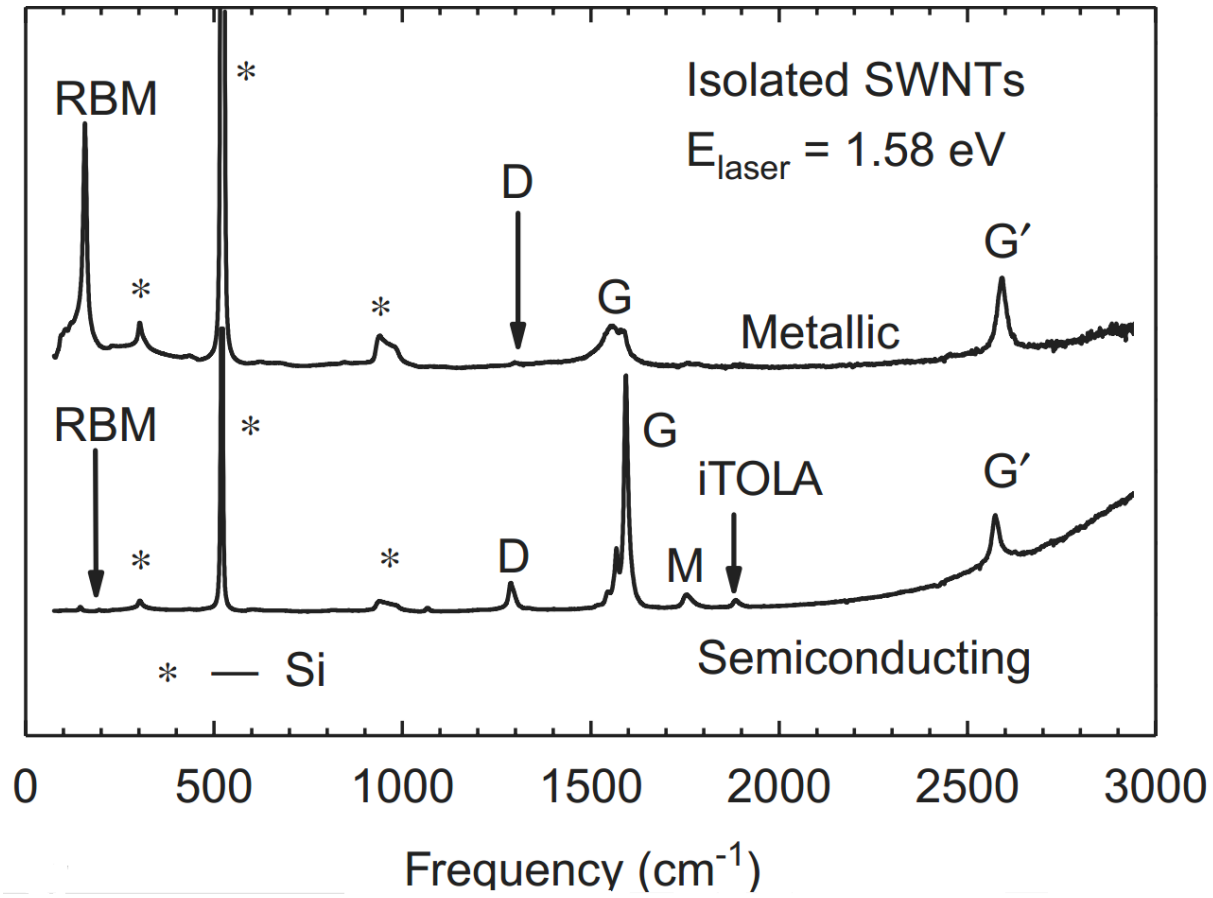

Figure 5 - Raman spectra of single-walled carbon nanotubes. Upper spectrum is of a metallic and lower of a semiconducting. [5]

2 Fabrication of microfluidic channels

The fabrication procedure follows heavily on the work and observations of Laura Rojas Rojas, as her work directly preceded this one [6]. The microfluidic channels were fabricated on to soda-lime glass chips by patterning the channels with electron beam lithography and etching the desired depth, finally sealing the channels through thermal fusion.

First the whole procedure with successful parameters is described, followed by a section with alternative methods and trials.

2.1 Glass and pretreatments

Glass chips used were Menzel-Gläser cover slips, made out of hydrolytic class 1 soda-lime glass. The cover slips were square, 20 mm x 20 mm in size and had thickness of 500 μm.[7] The composition of the glass is roughly 73% SiO_2, 14% Na_2O, 9% CaO, and 4% CaO with trace amounts of Al_2O_3, K_2O, $TiO_2$and Fe_2O_3. [8] Most of the processing is done to one 500 μm thick cover slip, called the channel chip. In the final phase one untreated coverslip is fused to the channel chip.

To each of the channel chips, four holes were drilled to act as liquid inlet/outlet holes. They were made by shooting a focused and pulsed laser beam to the glass until the laser went neatly through. The laser used was Lambda Physik OPTex excimer laser using KrF, thus having the wavelength of 248 nm. One pulse lasted for 8 ns, each having the energy of 14 mJ. The amount of pulses needed to make the holes was slightly above 1000, but shooting an extra 500 pulses made sure that the hole was uniform and took almost no extra time. The holes made this way had a diameter of 100 μm.

These steps was done in normal room conditions, but from here on the chips were transferred to ISO-5 cleanroom conditions to gain a control of surface cleanliness.

2.2 Metal mask

The channel chips were given a metal mask to enable electron beam lithography and on a later stage protect most of the surface from glass etching. Starting with channel chips with four holes, they were first cleaned in acetone, $(CH_3)_2CO$, using cotton sticks to remove larger trash particles. Acetone was rinsed with IPA (isopropanol, C_3H_8O), and blown dry with a nitrogen pistol. A second cleaning step was done in Piranha solution with composition of 1:3 of $H_2O_2 : H_2SO_4$. The Piranha cleaning was done for 10 minutes, rinsed in deionized water bath and sonicated in a fresh water bath for 3 minutes. After blowing the chip dry, it was ready for metal evaporation.

The metal mask was evaporated with Balzers BAE 250T evaporator. Evaporation speed was set between 1.0 Å and 1.6 Å, vacuum level reached was around $1 \cdot 10^{-5}$ mbar and the temperature was set by tap water cooling. The metal mask evaporated was 20 nm of chromium (Cr) and 40 nm of gold (Au).

2.3 Electron beam lithography

The shape of the microfluidic channels was drawn with electron beam lithography. For that purpose a resist mask is needed. The resist used was PMMA 950 A4, meaning Poly(methyl methacrylate) of molecular weight of 950 000 u is mixed as 4% in anisole,$CH_3OC_6H_5$. [9]

The channel chip with metal mask was placed on a hot plate of 160°C for 3 minutes to evaporate any residual humidity. The chip was then placed to a spinner, an excessive amount of PMMA pipetted on top of it and spun at 3000 rpm for 60 seconds. The chip

was then placed to the same hot plate for 3 minutes to bake the PMMA on the chip. The result will be a rather uniform layer of PMMA, having thickness of around 200 nm. [9]

The lithography was performed using Raith e_Line scanning electron microscope. The designed pattern consisted of circular exposures with the diameter of 500 µm at the inlet/outlet holes and rectangular design for the channels. The circular exposures near the holes ensured that the 100 µm drilled hole would certainly connect to the channels and let the liquid flow onwards. The electron beam writer was able to deliver a current of 7.6-8.2 nA and the exposed dose was 300 µAs/cm^2. Two of the designs exposed are shown in Figure 6.

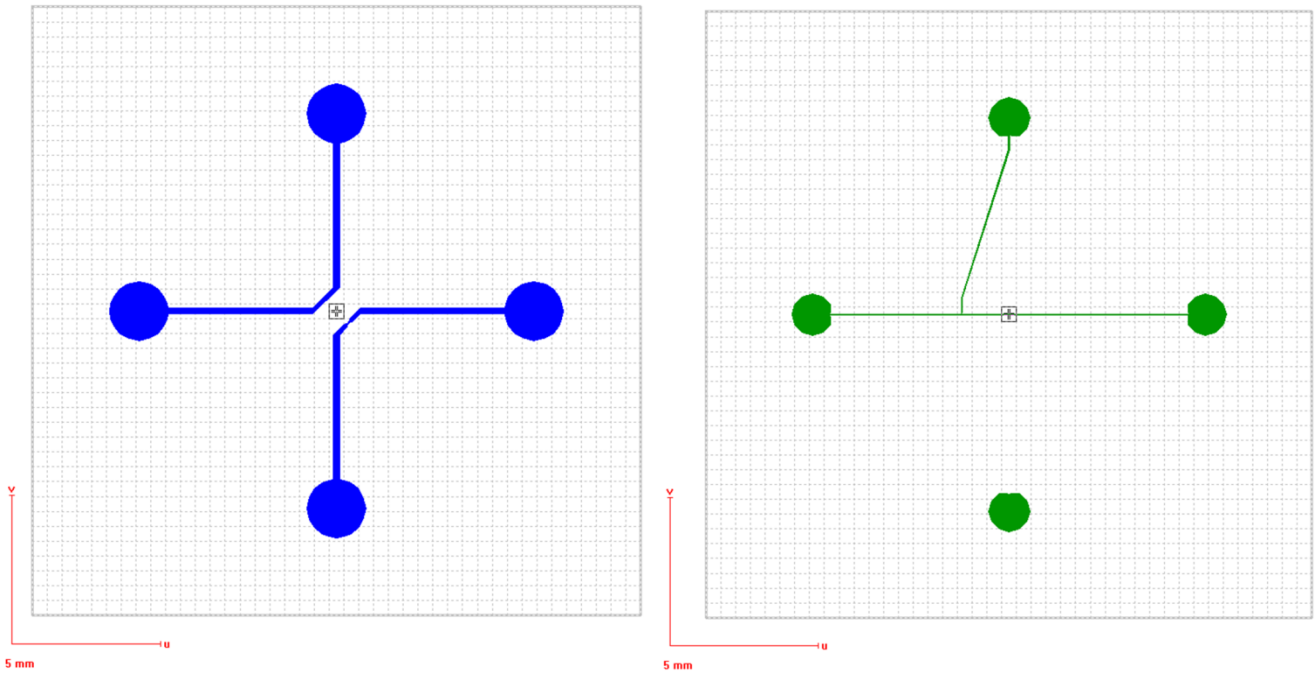

Figure 6 - Two of the channel designs. Left one shows 2 simple channels and the right one has a T-junction for droplet formation

After the exposure the chip was immersed in developer MIBK (methylisobutylketone) for 40 seconds, rinsed in IPA and blown dry with a nitrogen pistol. To enhance the protective function of the PMMA layer, the chip was hard-baked on a hot plate of 200°C for 90 minutes. Although this step rounds off small sharp features, the benefit of protection outweighed the sharpness. The rounding effect is shown in Figure 7.

Figure 7 - Effect of hard baking and etching to sharp features. The larger triangles are 10 μm in height and the smaller triangles have 5 μm height, channels are 50 μm wide.

2.4 Wet etching

The channel chip at this stage has chromium, gold and PMMA layers on most parts of the chip, and chromium and gold layers on the areas where the channels are designed. To etch the gold, aqua regia solution with the composition of 3:1:2 of $HCl\ (38\%) : HNO_3 : H_2O$ was used. The etching took around 1 minute to perform, after

which the chip was rinsed in water. The chromium etchant consisted of 1:3 solution of $NaOH(50\ g/100\ ml\ H_2O)$:$K[Fe_3(CN)_6]$ $(30\ g/100\ ml\ H_2O)$. After around 1 minute of etching, the sample was rinsed in water and had see-through portions where the channels will be.

The channel depth was etched with a mixture of hydrofluoric acid (HF) and hydrochloric acid (HCl). The etchant was diluted from 12:1 solution of HF (38%):HCl (38%) with water as in 1:6, so that the final concentrations were HF (6%):HCl (0.5%). This solution has a rather constant etch rate of 1 μm/minute. [6] The channel chip was immersed in the etchant for 4 minutes to obtain channel depth of 4 μm. HCl in the solution etches the minor components of soda-lime glass and thus helps to form a very smooth etched surface. After the HF etching, the chip was rinsed well in water.

The remainders of the PMMA layer were removed by a 5 minute acetone bath, rinsed in IPA and blown dry. The remaining metal masks could now be removed in the same etchants as before, first gold and finally chromium.

2.5 Thermal fusion of glass slides

As a pretreatment to both the processed channel chip and a clean, untreated glass chip of 500 μm thickness, a similar 10 minute Piranha cleaning step was performed as before the evaporation. The chips were rinsed in water, sonicated in new water bath for 3 minutes and blown dry.

The two chips were brought close together by hand and pressed tightly together as described by Renberg et al. [10] The chips were aligned such that the fabricated chan-

nels were left between the two chips, thus sealing the channels. In this stage even the smallest of dirt or trash particle or any gas trapped between the two glasses caused Newton rings to appear, centered on the particle or gas pocket. Most of these Newton rings could be removed by pressing the chips hard together while moving the fingers towards the edges. After repeating this pushing of Newton rings several times, only a few rings appeared just next to the trash particles, and any rings caused by trapped gas disappeared completely. Some rings may still exist due to a trapped particle, but if the rings didn't collide with the channels (see Figure 8), the sealing was good and ready for the finalization of the process.

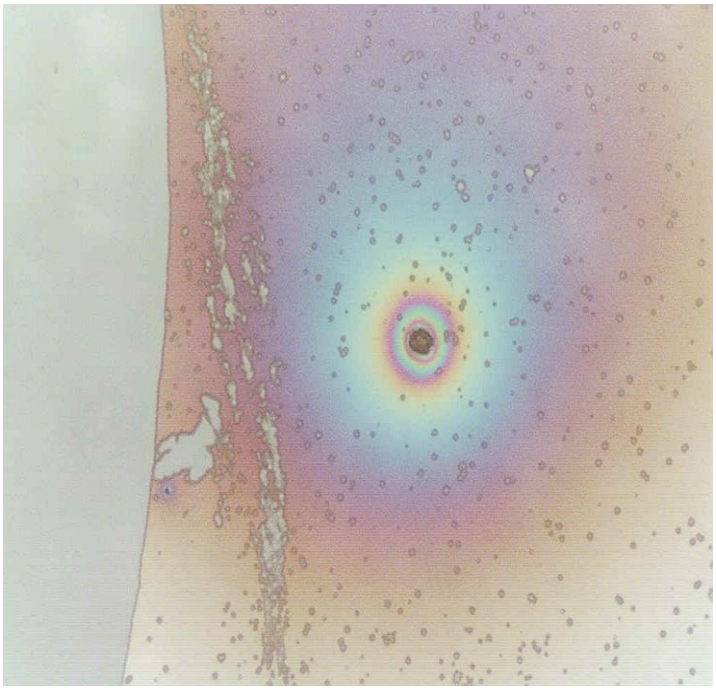

Figure 8 - Acceptable Newton rings due to a dust particle. The rings do not continue inside the channel visible to the left.

Thermal fusion of the glass slides was done with a programmable tube furnace MTI GSL-1100X, running a 710 Torr nitrogen atmosphere during operation. The glass slides were placed on a holder made out of brass. The holder had a lid with a 19.5 mm x 19.5 mm square pressure plate that pushed the glass slides tightly together by tightening the lid to the holder base with 4 screws. The holder was then placed to the middle of the furnace and the furnace was turned on. The program set to the furnace was 300 minutes to heat up to 580°C, 300 minutes to stay at 580°C and 300 minutes to cool down back to room temperature. After this procedure, the chip has sealed channels, ready for the microfluidic setup.

2.6 Alternative methods and trials

To achieve as thin samples as possible, 120 μm cover slips were first attempted to use as the channel chips. This caused several problems as such thin slides broke down very easily. Dropping the chip for a distance of few centimeters or even pressing it too tightly with the tweezers caused them to break into pieces. The thin slides were therefore quickly discarded from the use of channel chips.

Before using the laser to drill the holes, manual drilling with a Dremel hand drill equipped with a diamond tip of 1 mm in diameter was used for the inlet/outlet holes. Such handiwork isn't nearly as accurate as with the laser, causing the holes to be slightly in different positions each time. The holes were also quite big compared to the microfluidic channels. Finally, the drilling procedure caused many cover slips to have fractures and scratches along the surface causing this method to be forgotten and replaced by the laser.

Different compositions of the metal mask were investigated throughout the research. Other metals like copper, titanium or aluminum were adequate until wet etching phase as hydrofluoric acid etches those metals extremely fast, up to 1000 Å/min. [11] The amounts of chromium and gold were increased step by step as hydrofluoric acid slowly peels off all metals. Increasing the metal mask size to hundreds of nanometers would certainly provide enough protection, but that would also waste precious metals and time. Thus the optimal coverage for our purpose was found in the total mask size of 60 nm as described before.

In the attempt to make the metal mask survive the hydrofluoric acid treatment, liquid nitrogen cooling during the evaporation was also investigated to increase the uniformity of the metal layer. When comparing the evaporated layer with atomic force microscope, liquid nitrogen cooling did in fact reduce the amount of small bumps in the metal mask. However, the bumps still existed and were only a few nanometers at maximum. Additionally, a complication occurred after the evaporation as the extremely cold samples acquired an ice layer on top of them. Such cold samples became much more fragile and the removal of ice increased the amount of cleaning steps. In the end, liquid nitrogen cooling didn't provide the increased protection during the etching. Accounting for the extra time to set up the cooling system and the additional cleaning step, it was deemed much faster to just evaporate a thicker metal mask.

To help the last step of fabrication, the thermal fusion of glass slides, a pillar structure helping the gas to escape was experimented on as described by Stjernström and Roeraade. [12] The idea was to not only make channels for the liquid to pass, but also channels for gases that will be trapped between the glass slides and allow them to es-

cape from the sides of the slides. As the exposure was done with electron beam lithography, such a design over our sample effectively multiplied the exposure time needed by a factor of 6. This was still acceptable, but in the later processes the pillar structure didn't work as well as it was thought to. In the end, the problem was averted through other means and the pillar structure declared unnecessary.

Again to obtain thinner samples, 120 μm chips were attempted to use as the sealing chip in the thermal fusion. However, the Newton rings appearing were too much of a problem. If force was used in the attempt to remove the rings, the thinner glass slide could shatter. If only a little force was used, the rings persisted and created leaking channels. As no working samples were able to be fabricated using the 120 μm chips, they were abandoned.

3 Microfluidics

3.1 Microfluidic setup

The microfluidics was controlled using Fluigent MFCS-FLEX unit, running its original Maesflo software. The unit had 4 pressure outlets, two with 0-25 mbar, one with 0-69 mbar and one with 0-345 mbar output. The device uses a system called Fluiwell, which pushes nitrogen gas on top of a liquid reservoir, which has a Teflon tube inside the liquid. As the pressure increases on top of the liquid, it is pushed to the tube and from there to the microfluidic channel. The function is described in Figure 9.

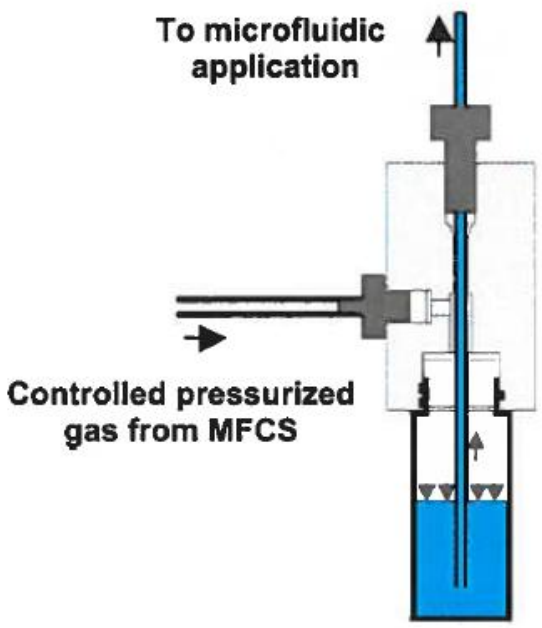

Figure 9 - The working principle of the Fluiwell setup[3]

As the microfluidic chips have 4 inlet/outlet holes, there can be 4 Teflon tubes attached to it. The tubes were round, having an inner diameter of 0.5 mm and an outer diameter of 1.6 mm. The length of each tube is from 20 cm to 30 cm. The other end of the tube is expanded by heating it out with Ismatec IC0043B tube-end expander. The expanded end is fitted with a small O-ring, which is then pressed against the inlet/outlet hole of the chip. As the chip is pressed against the O-rings, they flatten and prevent the liquid from escaping at the tube-chip intersection.

The chip, O-rings and the expanded ends of the tubes are inside a custom-made microfluidics holder made out of brass. The holder is somewhat similar than the one used in the thermal fusion, but this one is lighter and has a see-through portion at the

middle, enabling optical microscope observations of the fluid as well as Raman measurements at the channel.

3.2 Flow speeds at different pressures

The Teflon tubes connecting the liquid reservoirs and the microfluidic chip have the length of around 20 cm, allowing the macroscopic measurement of the flow speeds. The starting point of the fluid column is marked to the tube and then waited for a long time so that the reading error would be as little as possible. After we know the time and the distance it takes to travel it in the tube, the flow speed can be obtained from equation 5 and after that, channel speed from equation 2. The flow speed tests were done on a channel that is 200 μm wide and 4 μm deep with different pressures. The obtained speeds are shown in Table 1.

Pressure (mbar)	Time (h)	Distance (mm)	Flow rate (pl/s)	Channel speed (μm/s)
20	60.5	12	43	54
100	72	110.5	335	419
200	20.8	52	547	683
300	22	117.5	1165	1457

Table 1 - Flow speed calculations

With the lower pressures it is possible to go into flow speeds below 100 pl/s. This is still few orders of magnitude above our ultimate goal of femtoliter flow, but sufficient so far. At later stages this will cause problems as the channel speeds are so high and the channels themselves will get smaller, increasing the channel speed even more. As

the microfluidic controller might not be able to go into small enough speeds, another approach can be taken so that the liquid is moved and then stopped into measurement zone for the duration of Raman measurements.

3.3 Droplet formation

There are several ways to produce droplets inside a microfluidic channel. Our approach is to create an emulsion with oil and water, which are immiscible. The microfluidic channels form a T-junction and the two liquids are pushed to the junction at constant pressures. As they are immiscible, the flow of the one liquid is sheared by the other, forming droplets [13].

Figure 10 shows droplet formation with oil and water in 50 μm wide channels. The droplets then follow the channels with approximately the channel speed indicated in Table 1. After several droplets have been formed, they can be speeded up or slowed down by adjusting the pressure accordingly.

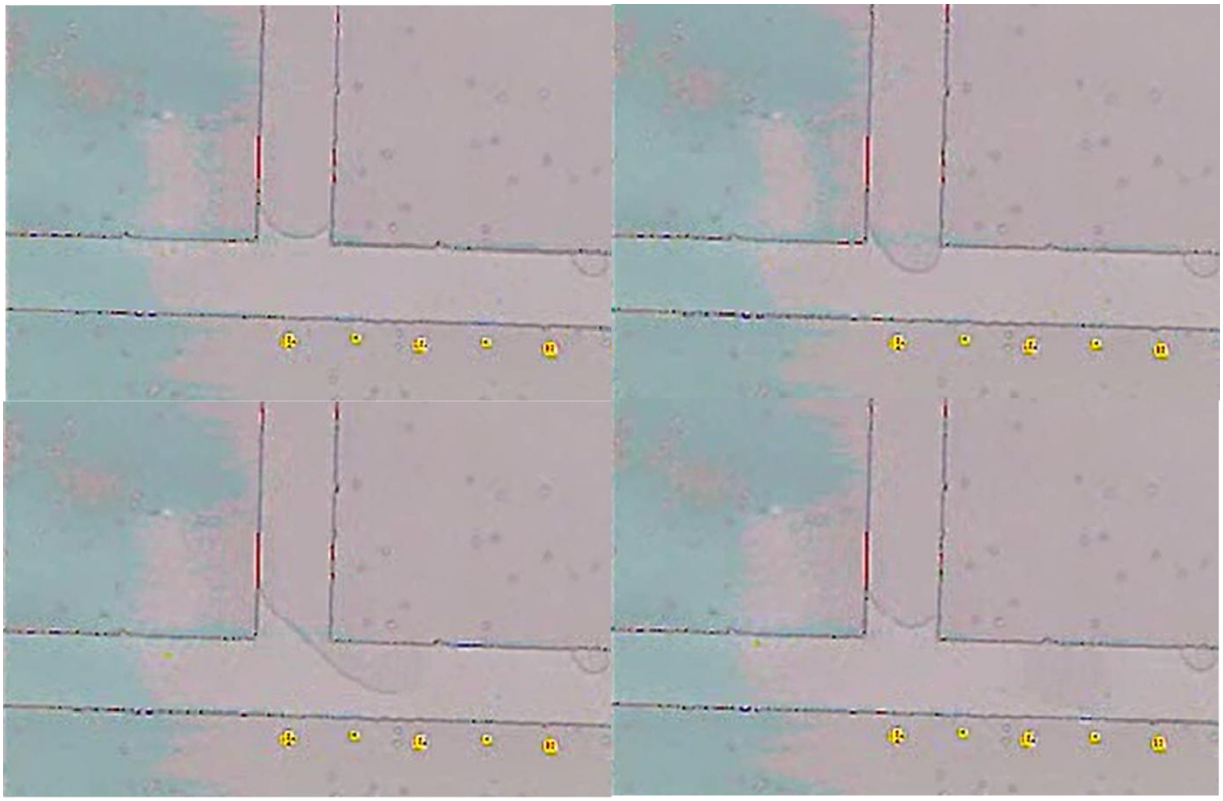

Figure 10 - Droplet formation in T-junction. Oil coming from upper channel is sheared by water flow. Picture contains color distortions from the imaging webcam.

4 Raman measurements

In the Raman measurement phase, pure water is now replaced with carbon nanotube solution. The nanotube material is rather concentrated, making every droplet to contain multiple carbon nanotubes. When too much of the material is in the same droplet, there is a possibility for the nanotubes to stack and eventually block the channel. Weak points for such blockage are the turning points; when the channels make a U-turn or a 90 degree turn. A blockage can be detected when the fluid can no longer pass through a certain point.

A good side with such a blockage is that we have a very high probability of finding carbon nanotubes inside of them. A sample with a blockage was mounted to the measurement setup, the laser was focused to the blockage, and the Raman spectrum measured. The measurement was background corrected, the Raman shift scanned up to 2200 cm^{-1} and light collected during 15 seconds. The resulting spectrum is shown in Figure 11.

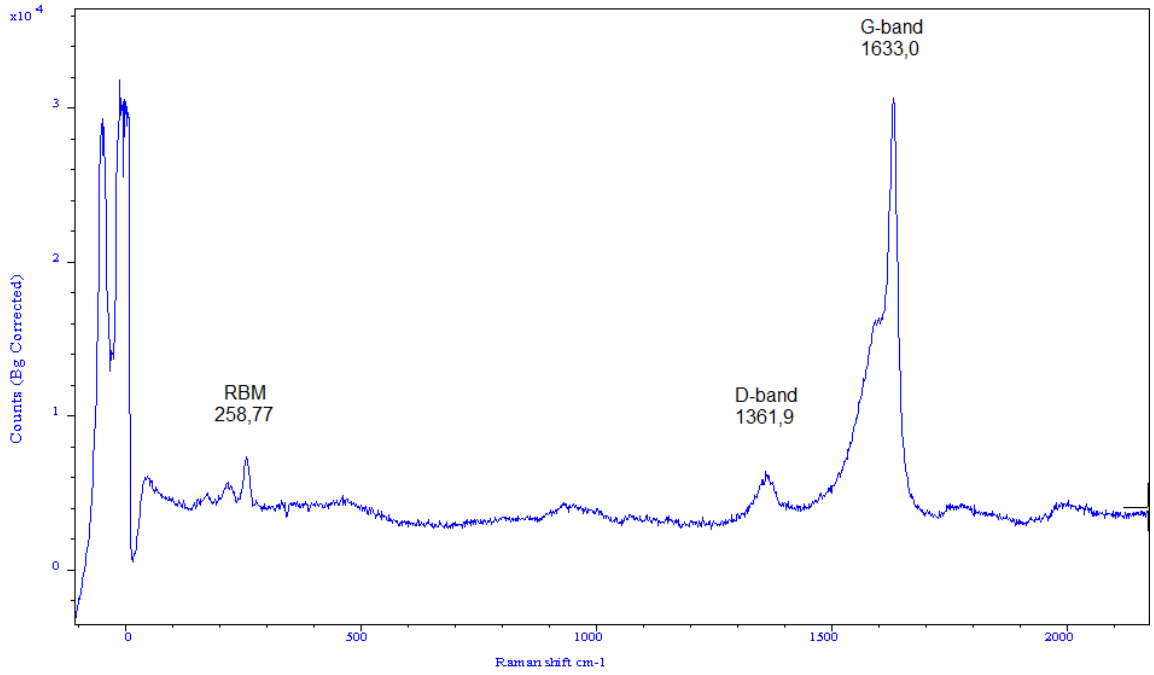

Figure 11 - Raman spectrum of carbon nanotubes in a blockage inside a channel

From it we can see that it has a highly peaked G-band and a clearly visible D-band. These are characteristic features of carbon nanotubes as seen in Figure 5, indicating that Raman signal of carbon nanotubes can be measured inside a microfluidic channel. However, there are several clear radial breathing modes also visible, showing that

there are multiple nanotubes present in the blockage. Therefore it would be challenging to distinguish between metallic and semiconducting nanotubes.

To get such smooth Raman spectra, the measurement time currently has to be rather long. Therefore the liquid flow has to be stopped before the measurement. If rougher spectra are acceptable, the measurement time can be reduced. With fast measurements and slow flow speeds it should be possible to reach continuous measurement with a constant flow speed.

5 Conclusions

With the fabrication steps figured out, the stage is set for more complex channel features. By using additional inlet/outlet holes it should be possible to fabricate sorter channeling after the measurement zone. Additionally with an extra inlet hole it should be possible to control backflow of the liquid also, as to push the liquid towards the beginning. However, this requires working with low pressures as the maximum pressures of the microfluidic controller need to be taken into account.

The channels have the tendency to get blocked rather easily after a bunch of carbon nanotubes are squeezed to them. This could later be averted by diluting the nanotube liquid and thus working with fewer and fewer tubes. This could eventually lead into capturing only one type or even capturing only a single nanotube. However, overdiluting will cause many measurements to have little value as no carbon nanotubes can be found. This calls for further experiments to find the optimal concentration.

In the droplet formation it is preferable that the walls of the channels would be hydrophobic so that the oil would be at the edges, shearing water droplets more easily. Most of the hydrophobic treatments are time-constrained such that in time, with available oxygen, the hydrophobic properties diminish and finally vanish. A more permanent solution would be to make a layer of hydrophobic molecules to the channels with for example atomic layer deposition. This will of course add steps to the fabrication part, but its worthwhileness could be investigated.

Now that the system is capable of measurements, the carbon nanotube liquid can be changed to almost any other interesting molecule or structure. Preferably the material should be small enough to easily fit into the channel, not stick to any neighboring materials and have a distinct Raman spectrum. Due to the difficulties of the system and the slow speed, this isn't ready for any industrial scaling, but rather will for now stay in the field of research.

Bibliography

[1] T. W. Odom, J. Huang, P. Kim and C. M. Lieber, "Structures and electronic properties of carbon nanotubes," *Journal of Physical Chemistry*, 2000.

[2] Arnero, "Wikmedia Commons," 29 November 2007. [Online]. Available: http://en.wikipedia.org/wiki/File:Carbon_nanotube_chiral_povray.PNG. [Accessed 3 May 2013].

[3] Fluigent, MicroFluidics Control System User Manual, Fluigent, 2008.

[4] Advanced Physics Laboratory, "Raman Spectroscopy," 2006.

[5] M. S. Dresselhaus, G. Dresselhaus, R. Saito and A. Jorio, "Raman Spectroscopy of Carbon Nanotubes," *Physics Reports,* 2004.

[6] L. Rojas, "Fabrication techniques for developing a functional microfluidic glass device suitable for detection in optical spectroscopy system," University of Jyväskylä, 2012.

[7] Menzel-Gläser, "Menzel-Gläser Cover slips," [Online]. Available: http://www.menzel.de/Cover_Slips.675.0.html?L=1. [Accessed 25 April 2013].

[8] T. P. Seward and T. Vascott, High temperature glass melt property database for process modeling, Ohio: The American Ceramic Society, 2005.

[9] MicroChem, "PMMA Data Sheet," 2001. [Online]. Available: http://microchem.com/pdf/PMMA_Data_Sheet.pdf. [Accessed 26 April 2013].

[10] B. Renberg, K. Sato, T. Tsukahara, K. Mawatari and T. Kitamori, "Hands on: thermal bonding of nano- and microfluidic chips," *Microchim acta,* vol. 166, pp. 177-181, 2009.

[11] K. R. Williams, K. Gupta and M. Wasilik, "Etch rates for micromachining processing - Part II," *Journal of Microelectromechanical systems,* vol. 12, no. 6, pp. 761-778, 2003.

[12] M. Stjernström and J. Roeraade, "Method for fabrication of microfluidic systems in glass," *Journal of Micromechanics and Microengineering,* vol. 8, pp. 33-38, 1998.

[13] H. A. Stone, A. D. Stroock and A. Ajdari, "Engineering flows in small devices: Microfluidics toward a Lab-on-a-Chip," *Annual Review of Fluid Mechanics,* vol. 36, pp. 381-411, 2004.